

MECHANISM OF THE FORMATION AND PROPERTIES OF ANTIMONY POLYPHOSPHATE

P. Melnikov^{1*}, F. J. dos Santos², S. B. Santagnelli², M. A. C. Secco¹, W. R. Guimarães¹, A. Delben¹ and J. R. Delben¹

¹Physics Department/CCET/UFMS, Caixa Postal 549, Campo Grande/MS, Brazil

²Institute of Chemistry, UNESP, Rua Prof. Francisco Degni s/n, CP 355, CEP 14801-970, Araraquara, SP, Brazil

Formation of antimony polyphosphate using Sb_2O_3 and/or $(\text{NH}_4)_2\text{HPO}_4$ and $\text{NH}_4\text{H}_2\text{PO}_4$ as starting materials has been simulated by thermal analysis technique. The elimination of water and ammonia molecules induced by heating leads to the formation of intermediate ammonium polyphosphate, which subsequently reacts with Sb_2O_3 . Morphologically, vitreous $\text{Sb}(\text{PO}_3)_3$ is composed of plaques having irregular shapes. Infrared spectra and NMR study is consistent with tetrametaphosphate anion arrangement. The compound is thermally unstable and may be recommended as a donor of $-\text{O}-\text{P}-\text{O}-$ linkers in the preparation of special phosphate glasses.

Keywords: antimony, glasses, inorganic materials, polyphosphate

Introduction

Currently polyphosphates of trivalent elements, rare earths in particular, are widely employed in phosphate glasses suitable for high tech optical devices, photonics and biomedical engineering. The difficulty consists, however, in the fact that rare earth content should not exceed certain limits (generally less than 5%). In a luminescent material, for example, the emission may be severely quenched by an excessive lanthanide concentration. At the same time, the amount of phosphorus required may be higher than introduced in the form of starting polyphosphate. The desirable situation is to correct batch composition by addition of a precursor containing optically neutral cation, whose ionic radius is close to that of the lanthanide employed. In this sense, antimony polyphosphate seems to be the best candidate since its ionic radius (90 pm) is the closest to those of optically active lanthanides of erbium subgroup (near 100 pm). An additional advantage consists in a lower stability of antimony compounds, so they split easily giving rise to free $-\text{O}-\text{P}-\text{O}-$ bridges that may act as structure linkers. Because of these units glass domains in polyphosphate systems are wider and glass compositions more stable [1]. However, according to available published data, antimony polyphosphate has not attracted much attention from researchers. Its preparation from Sb_2O_3 , $(\text{NH}_4)_2\text{HPO}_4$, $\text{NH}_4\text{H}_2\text{PO}_4$ and NH_4NO_3 was first mentioned in a patent description [2], but a technique comprising the usage of NH_4NO_3 is seriously

limited because of its oxidative properties and technological hazards. Moreover, the stoichiometry $\text{Sb}:\text{P}=1:3$ is not guaranteed at the conditions recommended in the patent and the final product may be contaminated. Another method, using H_3PO_4 as phosphorus source, permits to the formation of high quality crystalline antimony polyphosphate [3], but it is applicable only to the preparation of relatively small samples. In this case, initial deposits of polyphosphate which are being formed on the oxide grain surface would block further interaction and therefore the reaction product would contain a variety of phases including antimony oxide. The aim of the present work is to study the mechanisms of formation and some properties of $\text{Sb}(\text{PO}_3)_3$. As shown in recent publications it may be successfully done using thermal analysis in association with other instrumental techniques [4, 5].

Experimental

Starting reagents were ammonium hydrogen phosphate $(\text{NH}_4)_2\text{HPO}_4$ (Merck), ammonium dihydrogen phosphate $\text{NH}_4\text{H}_2\text{PO}_4$ (Synth) and antimony(III) oxide (Merck), all of analytical grade purity. $\text{Sc}(\text{PO}_3)_3$ was specially prepared according to [6]. Thermal behavior was studied by differential thermal analysis (DTA) and thermal gravimetric analysis (TG) (both 50H Shimadzu Instrumentation). Preparations were simulated by mixing up starting materials and heating the test specimens (4–6 mg) up to 900°C in the flux of

* Author for correspondence: petrmelnikov@yahoo.com

synthetic air at the rate $10^{\circ}\text{C min}^{-1}$. Mass losses during heating were analyzed and compared to previously calculated values. Chemical analysis for Sb and P was carried out by ICP technique with multi-element standard solution IV, Merck AG. Scanning electron microscopy (SEM) was carried out using a SM-300-TOPCON instrument. Energy dispersive analysis (EDAX) was performed using a Princeton Gamma Tech PGT instrument provided with SiLi detector. X-ray diffraction patterns were registered with a Siemens Kristalloflex diffractometer with a graphite diffracted beam monochromator and Ni filter. MAS NMR spectra were recorded on an INOVA Varian-300 spectrometer working at 121.442 MHz (^{31}P), spinning frequency of 5000 Hz, a pulse length of $\pi/2$ and a repetition time between acquisitions of 90 s, the reference at 0 ppm being taken as H_3PO_4 at 85%. The samples were previously ground into powders and used to fill a zirconia tube. IR spectra were recorded on a FT-IR Spectrophotometer Spectrum 2000. Samples must be processed immediately since even 20 min exposure to ambient air is enough to change the IR spectra.

Results and discussion

Thermal analysis

The TG curve of the mixture $\text{NH}_4\text{H}_2\text{PO}_4\text{-Sb}_2\text{O}_3$ (Fig. 1) shows two mass losses at 200 (11%) and 488°C (14.9%) accompanied by two endothermic effects at the same temperatures, which suggests $\text{Sb}(\text{PO}_3)_3$ does not form directly and an intermediate condensation is hypothesised. Calculated values for mass losses fit the following reaction scheme



The TG and DTA simulations for samples containing $(\text{NH}_4)_2\text{HPO}_4$ and Sb_2O_3 (Fig. 2) are more complex. Consider the entire reaction,

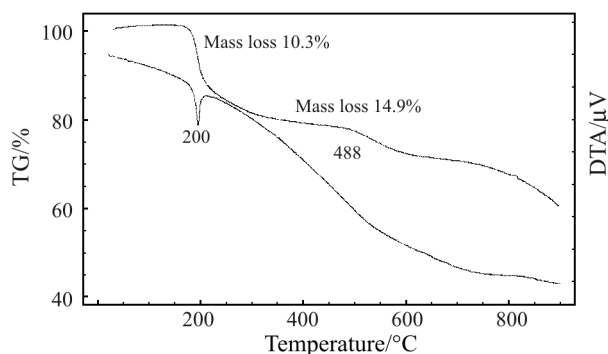


Fig. 1 DTA and TG curves simulating $\text{Sb}(\text{PO}_3)_3$ preparation from $\text{NH}_4\text{H}_2\text{PO}_4$ and Sb_2O_3

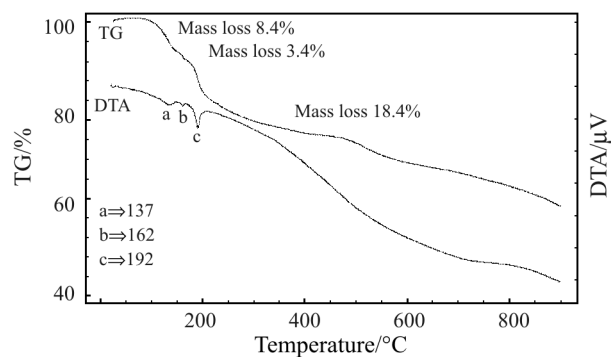


Fig. 2 DTA and TG curves simulating $\text{Sb}(\text{PO}_3)_3$ preparation from $(\text{NH}_4)_2\text{HPO}_4$ and Sb_2O_3



Two of the first mass losses and endothermic effects, correspond to the elimination of $3\text{H}_2\text{O}$ and 3NH_3 (*calc.* 9.3%; *exp.* 8.4%) and the third (*calc.* 4.5%; *exp.* 3.4%) corresponds to elimination of 3 additional NH_3 . This suggests the condensation process:



At the fourth step, $3\text{H}_2\text{O}$ and 6NH_3 are eliminated (*calc.* 18.6%; *exp.* 18.4%), so that the interaction process between $(\text{NH}_4\text{PO}_3)_n$ and Sb_2O_3 remains the same. Note the differences between calculated and experimental values, which in the latter are larger than in the former. Possibly the slower decomposition of $\text{NH}_4\text{H}_2\text{PO}_4$ with partial trapping of ammonia in the (NH_4PO_3) network is responsible. The absence of a pronounced endothermic effect, associated with melting, suggests the polymeric nature of $\text{Sb}(\text{PO}_3)_3$. TG curves show that in both cases mass loss does not stop after 480°C , suggesting either polyphosphate evaporation or its decomposition.

When experiments are carried out in open crucibles a white porous mass forms at $\sim 450^{\circ}\text{C}$, which around 480°C softens, becoming a somewhat purplish liquid. The solid obtained from the melt by fast cooling is a translucent brittle glass-like material. Chemical analysis rendered the following values: *Calcd.* for $\text{Sb}(\text{PO}_3)_3$ (%): Sb, 33.92; P, 25.93. *Found:* Sb, 33.18; P, 26.00. X-ray patterns show that the product is amorphous, so we are really dealing with a glass form of antimony polyphosphate.

The compound is extremely hygroscopic and has to be sealed in a glass ampoule immediately after its preparation. The samples become wet after being exposed to air for 20–30 min. In water they are rapidly hydrolyzed giving a suspension of a white crystalline substance, which was identified by X-ray patterns as antimony(III) orthophosphate, SbPO_4 (ICDD file 23-2793) contaminated with antimony(V) oxophosphate SbOPO_4 (ICDD file 40-0037).

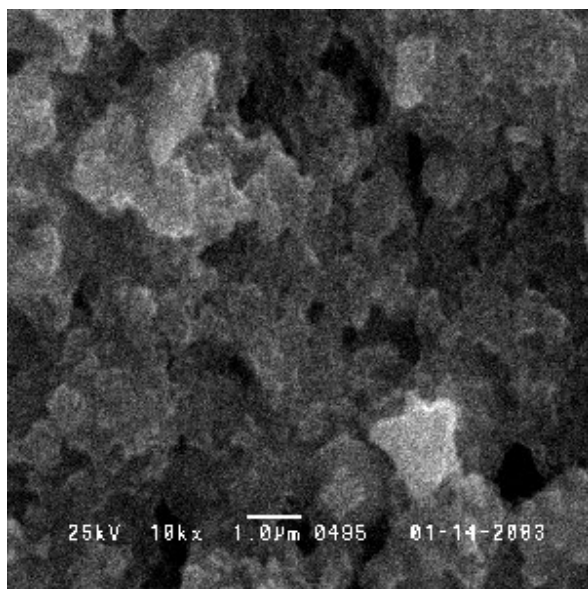


Fig. 3 SEM image of the $\text{Sb}(\text{PO}_3)_3$ glass form

The SEM photograph of the $\text{Sb}(\text{PO}_3)_3$ glass (Fig. 3) shows plates or laminas of irregular form with dimensions of about $1.1 \cdot 0.2 \mu\text{m}$. They tend to form larger aggregates, all of them placed in a parallel manner with respect to the crucible bottom, except for the only one located in the left upper quadrant of the image, which looks transversal to the others. Thus glass morphology seems to indicate that the structure is rather anisotropic. Black interstitial regions correspond to micropores in the glass. Energy dispersive X-ray spectrum of the sample given in Fig. 4 has been chosen as the most representative among those taken to characterize the vitreous antimony polyphosphate. It is dominated by the K_α and L_α lines of antimony and phosphorus. Oxygen is poorly detected by this method, its peak corresponds to a shoulder at the base of phosphorus signal reflecting a lower energy level. Nickel peaks are artifacts originating from the detector material.

Thermal stability of $\text{Sb}(\text{PO}_3)_3$ is much lower than that of lanthanide polyphosphates $\text{Ln}(\text{PO}_3)_3$ [6]. It

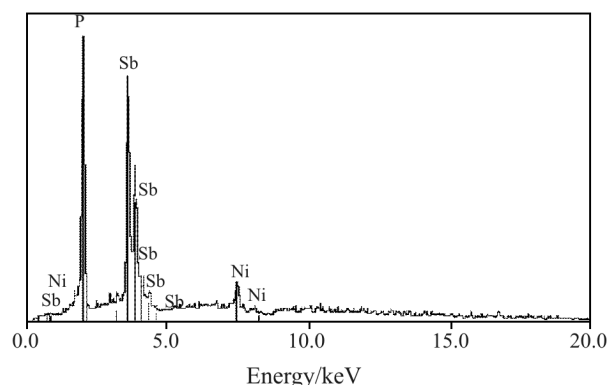


Fig. 4 Energy dispersive X-ray spectrum of $\text{Sb}(\text{PO}_3)_3$ glass form

starts to decompose just after being melted, at 480°C when the bubbles going upwards are observed.

The SEM image of the quenched sample (Fig. 5) resembles the surface of a boiling liquid showing that the aforementioned parallel plates have been transformed into spherulites with a diameter ca $2.5\text{--}3.0 \mu\text{m}$. They move upwards and burst upon reaching the upper boundary. Chemical analysis shows that the relation Sb:P (initially equal to 0.33) increases with the heating time, so it can be concluded that the product is being enriched in Sb, the gaseous phase being actually P_2O_5 . This means that when needed, $\text{Sb}(\text{PO}_3)_3$ may be used as the provider of $-\text{O}-\text{P}-\text{O}-$ linkers at relatively low temperatures and that the remaining form of antimony would be chemically neutral SbPO_4 . An additional advantage of the decomposition process is that P_2O_5 would act as a mechanical agitator making the diffusion more complete.

It is difficult to form an estimate of structural characteristics when the X-ray diffraction pattern is missing. So we tried an indirect approach, using spectroscopic data of a compound whose IR spectra is similar to $\text{Sb}(\text{PO}_3)_3$ and at the same time whose structure is resolved. In order for that to happen scandium polyphosphate (form A) has been synthesized and its IR spectra registered. The main idea was to benefit from the similarities of Sc and Sb ionic radii (88.5 and 90.0 pm respectively). Surely, in this case we shall get the information exclusively about the anion involved.

$\text{Sb}(\text{PO}_3)_3$ vibration frequencies are shown in Table 1 in comparison with those of $\text{Sc}(\text{PO}_3)_3$. Assignments have been made on the basis of the vast amount

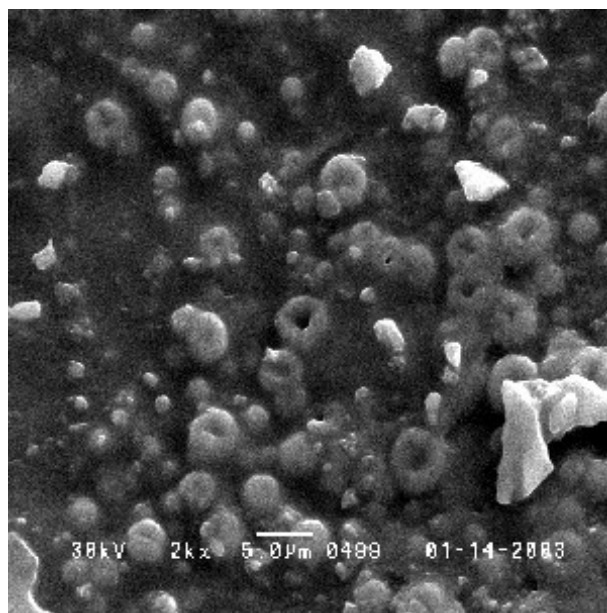


Fig. 5 SEM image of the quenched $\text{Sb}(\text{PO}_3)_3$ glass. White rhodium of irregular form seen in the photograph are metallic particles mixed in for noise control

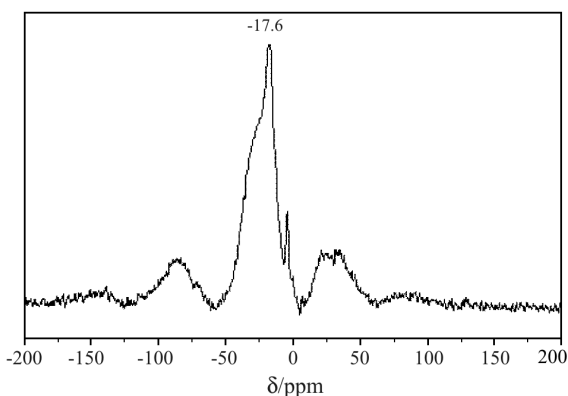
Table 1 Infrared absorption (cm^{-1}) of $\text{Sb}(\text{PO}_3)_3$ and $\text{Sc}(\text{PO}_3)_3$

Frequencies $^*/\text{cm}^{-1}$		Assignments [6–9]
$\text{Sb}(\text{PO}_3)_3$	$\text{Sc}(\text{PO}_3)_3$	
1258 vs	1254 vs	$\nu_{\text{as}}(\text{O}^- - \text{P} - \text{O}^-)$
–	1113 w	$\nu_{\text{s}}(\text{O}^- - \text{P} - \text{O}^-)$
1092w	1081w	
1007 w	1023 w	$\nu_{\text{as}}(\text{P} - \text{O} - \text{P})$
920 s	952 s	
714 s	717 s	$\nu_{\text{s}}(\text{P} - \text{O} - \text{P})$
641 m	682 m	$\delta(\text{P} - \text{O} - \text{P})$
–	611 m	
–	542 sh	
510 vs	507 vs	$\delta(\text{P}_4\text{O}_{12})$
420 m	424 m	
406 w	407 w	$\nu(\text{Me(III)} - \text{O})$

*vs, very strong; s, strong; m, medium; sh, shoulder; w, weak

of published polyphosphate spectra. According to these comparative data, the vibrational modes of both compounds closely resemble each other. Small disagreements in the values of $\nu_{\text{s}}(\text{O}^- - \text{P} - \text{O}^-)$ and $\nu_{\text{as}}(\text{P} - \text{O} - \text{P})$ may be due to the differences in covalency of scandium and antimony. They are not uncommon for polyphosphates that admit a wide range of distortions within phosphorus tetrahedra with the consequent repercussions in the angles and bond lengths values [9]. Hence, the available data on structure determination [10] allows considering the anion as a tetrametaphosphate cycle. The cationic network remains unknown; in any case for vitreous samples it should be largely disordered and difficult to identify.

NMR spectrum of antimony polyphosphate (Fig. 6) confirms this supposition. It resembles the spectra of alumophosphate glasses [11] and Na–Sr-phosphate glass-ceramics [12]. Although making unambiguous assignments for ^{31}P is difficult because of the apparent presence of multiple, overlapping resonances, the strongest peak at 17.8 ppm can

**Fig. 6** Antimony polyphosphate ^{31}P NMR spectrum

be assigned to Q^2 species. This means that a single unit has two bridging phosphorus atoms forming metaphosphate cycles. It also makes comprehensible the mere existence of a vitreous modification: large bi-dimensional ‘molecular’ groups (based on Q^2 tetrahedra) are continually undergoing geometrical changes and inhibit crystallization exactly in accordance with an earlier Hägg’s idea [13]. The decrease in shielding – or more positive chemical shift – in comparison to the widespread range -18.8 – 22.5 ppm additionally indicates a low grade of anion polymerization, suggesting (as also IR spectra do), a tetrametaphosphate rather than polymetaphosphate character of the cycles.

Unfortunately, in the field of material science the properties of $\text{Sb}(\text{PO}_3)_3$ as P_2O_5 provider are frequently underestimated. Care should be taken when analyzing systems with polyphosphates. An example is a recently published paper [14] where new films based on the binary system $0.20\text{Sb}(\text{PO}_3)_3$ – $0.80\text{Sb}_2\text{O}_3$ are described. However, evidence suggests that under these conditions $\text{Sb}(\text{PO}_3)_3$ would have reacted with antimony oxide according to the reaction



rendering antimony orthophosphate. So the binary system in actual fact is not $0.20\text{Sb}(\text{PO}_3)_3$ – $0.80\text{Sb}_2\text{O}_3$ but 0.2SbPO_4 – $0.6\text{Sb}_2\text{O}_3$, that consists of antimony orthophosphate containing excessive quantities of oxide. Undoubtedly, that seriously alters the interpretations, in particular the assignments of IR spectra.

Conclusions

Antimony polyphosphate synthesis is a complex process that compulsorily includes an intermediate formation of $(\text{NH}_4\text{PO}_3)_n$. The best phosphorus source when preparing $\text{Sb}(\text{PO}_3)_3$ is $\text{NH}_4\text{H}_2\text{PO}_4$ and not $(\text{NH}_4)_2\text{HPO}_4$. $\text{Sb}(\text{PO}_3)_3$ glass-like modification is a stable product formed by parallel plaques of irregular shape. Infrared spectra and NMR study suggest that the anionic network containing Q^2 species is based on labile tetrametaphosphate cycles, which restrain the crystallization and explain the stability of a vitreous phase. Thermal behavior of the compound is consistent with polymeric arrangement.

References

- 1 N. E. Alexeev, V. P. Gapontsev and M. E. Szabotinskii, ‘Laser Phosphate Glasses’, Nauka, Moscow 1980.
- 2 N. M. Sergueeva, L. N. Urusovskaya, A. I. Teterevkov, V. V. Androsik and A. N. Klimenkova, Patent SU, n° 1216150, C01 B 25/44, 27 July 1986.

- 3 P. Melnikov, Marcel Poulain, Michel Poulain, S. Ripeiro and P. P. Corbi, Patent France, n° 2794740, C01 B 25/44, C01G30/00, CO3C3/247, CO4B35/447, 15 December 2000.
- 4 S. Garnier, S. Petit and G. Coquerel, *J. Therm. Anal. Cal.*, 68 (2002) 489.
- 5 L. Stoch, *J. Therm. Anal. Cal.*, 77 (2004) 7.
- 6 P. P. Melnikov, L. N. Komissarova, T. S. Romanova and A. K. Stepanov, *Inorg. Mater.*, 12 (1976) 877.
- 7 N. N. Chudinova, L. N. Komissarova, P. P. Melnikov, *et al.*, "Rare Earth Compounds, Silicates, Germanates, Phosphates, Arsenates, Vanadates", Nauka, Moscow 1983.
- 8 L. P. Mezentseva, A. I. Domanskii and I. A. Bondar, *Zh. Neorg. Chim.*, 22 (1977) 84.
- 9 B. N. Litvin and V. A. Maslobojev, 'Rare Earth Phosphates', Nauka, Leningrad 1989.
- 10 M. Bagieu-Beucher and C. Guitel, *Acta Cryst.*, B. 34 (1978) 1439.
- 11 J. M. Egan, R. M. Wenslow and K. T. Mueller, *J. Non-Cryst. Solids*, 261 (2000) 115.
- 12 R. A. Pires, I. Abrahams, T. G. Nunes and G. E. Hawkes, *Key Engineering Mater.*, 254-256 (2004) 95.
- 13 R. K. Brow, *J. Non-Cryst. Solids*, 263-264 (2000) 1.
- 14 F. S. De Vicente, M. Siu Li, M. Nalin and Y. Messaddeq, *J. Non-Cryst. Solids*, 330 (2003) 168.

Received: September 1, 2004

In revised form: December 16, 2004

DOI: 10.1007/s10973-005-6420-6